

Observation of elliptic incoherent spatial solitons

Omer Katz, Tal Carmon, Tal Schwartz, and Mordechai Segev

Department of Physics and Solid State Institute, Technion, Haifa 32000, Israel

Demetrios N. Christodoulides

School of Optics, Center for Research and Education in Optics and Lasers, University of Central Florida, Orlando, Florida 32816-2700

Received November 16, 2004

We present the first experimental observation of spatially incoherent elliptic solitons. We use partially spatially incoherent light with anisotropic correlation statistics and observe elliptic solitons supported by the photorefractive screening nonlinearity. © 2004 Optical Society of America

OCIS codes: 190.5940, 190.4420, 222.0220, 220.4000.

Optical spatial solitons, which are self-trapped beams that exhibit particlelike behavior, have been the topic of extensive investigation for more than 30 years.¹ Self-trapping of coherent optical beams occurs when linear diffraction is exactly balanced by self-focusing as a result of optical nonlinearity. When the nonlinearity is saturable, it can support solitons that are trapped in both transverse dimensions, forming (2 + 1)D solitons.² Such solitons are generically circularly symmetric in all (saturable) nonlinear media for which the nonlinearity is isotropic with respect to the transverse directions. Indeed, (2 + 1)D solitons with circular (axially symmetric) wave functions have been observed in a variety of saturable nonlinear media (see, e.g., Refs. 3–7). These solitons are generally very robust entities; hence they form and attain their circular shape even if the input beam is slightly elliptic.⁸ If, however, a highly elliptic coherent beam is launched into a saturable self-focusing medium, it cannot form a soliton; that is, its propagation dynamics is never stationary. Instead, such a coherent elliptic beam develops periodic oscillations in its two different widths, with different oscillation periods, as was shown theoretically^{9,10} and experimentally.¹¹ The reason behind such oscillatory propagation dynamics associated with coherent elliptic beams in isotropic (and saturable) self-focusing media is as follows: To support a soliton, the nonlinearity must exactly balance the diffraction of a beam. The strength of the nonlinearity is set by the peak intensity of the beam. Hence, for a circular beam, the beam's intensity determines the width of the soliton that the beam can form or, equivalently, the diffraction angle that this change in nonlinear index can balance. This implies that only beams that diffract in an axially symmetric fashion can form solitons in isotropic nonlinear media. On the other hand, elliptic beams have elliptic plane-wave spectra, and consequently they diffract at different angles in their transverse directions (experiencing more broadening in their narrow direction). Thus coherent elliptic beams cannot form solitons in isotropic nonlinear media because such nonlinearities cannot compensate for two different diffraction angles simultaneously.

Whereas diffraction of monochromatic coherent beams is determined solely by the beam width, diffrac-

tion of incoherent beams offers an additional degree of freedom. That is, the diffraction of a partially spatially incoherent beam is determined by both its correlation statistics (manifested in its finite spatial correlation distance) and its width (in wavelength units). One can therefore engineer the properties of partially incoherent light such that spatially incoherent elliptic beams have isotropic plane-wave (power) spectra; i.e., the far field of such a beam is circular. Consequently, based on the experimental and theoretical knowledge of incoherent solitons accumulated in the past seven years^{12–18} it is possible to generate elliptic incoherent solitons^{19–22} by launching properly designed elliptic beams with anisotropic coherence properties into an isotropic noninstantaneous nonlinear medium.

Here we present the first experimental observation of elliptic incoherent spatial solitons. We show that when the correlation function of such an elliptic beam is appropriately made anisotropic, the beam has a circular far field, as opposed to its coherent counterpart that has an elliptic far field. Consequently, such an elliptic partially spatially incoherent beam can self-trap in a noninstantaneous, saturable, nonlinear medium and form an elliptic soliton. Our elliptic solitons are supported by the photorefractive screening nonlinearity.^{5,8,23–25} We also demonstrate that the self-trapping effects underlying the elliptic solitons do not arise from the residual anisotropy associated with screening nonlinearity.

The main challenge in our experiment is to engineer a partially spatially incoherent elliptic beam with a circular spatial spectrum (far field). Our technique involves two steps. In the first step we create a spatially incoherent beam with a highly eccentric elliptic profile but with isotropic correlation statistics, that is, an elliptic beam that is composed of randomly varying circular speckles. In the second step we demagnify the beam with a different demagnification in each of the ellipse's axes, thus creating a less-eccentric elliptic profile but with anisotropic correlation statistics. The outcome is an elliptic beam made from elliptic speckles, with the major axis of the speckles parallel to the minor axis of the beam. That is, the elliptic beam is more coherent in its narrow (near-field)

axis and less coherent in its long axis. When it is properly designed, such an elliptic spatially incoherent beam can have a circular far-field diffraction pattern.

The experimental setup is shown in Fig. 1. A 488-nm cw argon-laser beam is split by a polarizing beam splitter. The ordinarily polarized beam is expanded and used as the background beam as necessary for photorefractive screening nonlinearity.⁵ The extraordinarily polarized beam is made elliptical and highly eccentric [by means of two cylindrical lenses with foci $f_1^{(x)} = 10$ cm and $f_2^{(y)} = 3$ cm] and is incident in this form onto a rotating diffuser located at the focal plane of both cylindrical lenses. When this beam passes through the rotating diffuser, it becomes partially spatially incoherent.¹² The rotating diffuser is mounted on a sliding track that enables us to alternate between a spatially coherent and a partially spatially incoherent state without changing the elliptic shape of the beam. At this stage the elliptic beam has isotropic correlation statistics, as it is constructed from circular speckles. Then, we demagnify this elliptic beam in a telescopic imaging system with different demagnifications in the transverse directions (0.8 and 0.5 in the y and x directions, respectively). We do so by means of two pairs of different cylindrical lenses [$f_3^{(y)} = 25$ cm, $f_5^{(y)} = 20$ cm, $f_4^{(x)} = 30$ cm, $f_6^{(x)} = 15$ cm], with the diffuser located at the front focal planes of f_3 and f_4 (Fig. 1). Notice that the sum of the focal lengths in x is equal to that in y , i.e., $f_3^{(y)} + f_5^{(y)} = f_4^{(x)} + f_6^{(x)} = 45$ cm, to produce a common beam waist at the same plane (which will serve as the input plane to the nonlinear medium). The end result is a beam with an elliptic intensity profile but with anisotropic correlation statistics such that the beam is more coherent in the direction of its narrow (near-field) width. The beam is then recombined with the background beam, and both are sent through a photorefractive $\text{Sr}_{0.6}\text{Ba}_{0.4}\text{Nb}_2\text{O}_6$ (SBN) crystal. Self-focusing occurs with the application of an appropriate field (magnitude and polarity), which gives rise to a space-charge field with a large component along the c axis, to create the index change required for self-trapping. We monitor the intensity distribution of the extraordinary polarized beam at the input and output faces of the crystal with a CCD camera.

As a first step we measure the free-space diffraction (FWHM; Fig. 2). We find that the coherent elliptic beam (with the diffuser removed) of widths $\Delta x = 29 \mu\text{m}$ and $\Delta y = 17 \mu\text{m}$ [Fig. 2(a)] diffracts, after 5 mm of propagation in free space, to an elliptic shape rotated by 90° , with widths $\Delta x = 46 \mu\text{m}$ and $\Delta y = 73 \mu\text{m}$ [Fig. 2(b)]. Inserting the diffuser, thus making the beam partially spatially incoherent (as described above), caused the linear free-space diffraction pattern to become circular [Fig. 2(c)], with widths $\Delta x = 90 \mu\text{m}$ and $\Delta y = 83 \mu\text{m}$. We estimate the spatial correlation distance of our incoherent elliptic beam from its far-field diffraction by using the convenient formula in Ref. 20, which assumes a Gaussian correlation function. We find the correlation distances along the transverse axes to be $l_{cy} \approx 25 \mu\text{m}$ and $l_{cx} \approx 16 \mu\text{m}$.

We next insert the 6-mm-long crystal into the setup and launch the elliptic beam into it such that the long (major) axis of the ellipse is parallel to the direction of the applied field. Figure 3 shows the self-trapping results. The input beam [Fig. 3(a)] is $\Delta x = 29 \mu\text{m}$, $\Delta y = 17 \mu\text{m}$. The elliptic soliton forms at 1.1 kV/cm, as shown by the self-trapped output beam with widths $\Delta x = 28 \mu\text{m}$ and $\Delta y = 17 \mu\text{m}$ [Fig. 3(b)]. For comparison, Fig. 3(c) shows the linearly diffracted output beam of $\Delta x = 44 \mu\text{m}$ and $\Delta y = 42 \mu\text{m}$, which is almost ideally circular (as in free space). At this point it is essential to show that the elliptic incoherent solitons do not arise from the residual anisotropy associated with the screening nonlinearity. In some photorefractive crystals (e.g., $\text{Bi}_{12}\text{TiO}_{20}$, $\text{Bi}_{12}\text{SO}_{20}$, and $\text{Bi}_{12}\text{GeO}_{20}$, the anisotropy is fairly large,²⁶ but in SBN, which is the most commonly used material for generating photorefractive screening solitons, the anisotropy is small.^{8,27} Nevertheless, it is important to confirm that indeed the elliptic incoherent solitons do not arise from the residual anisotropy. To show this, we rotate the beam by 90° , such that the applied field becomes parallel to the short (minor) axis of the elliptic input beam. Repeating the self-trapping experiment, we achieve similar results [Figs. 3(d)–3(f); the transverse coordinates were chosen such that x was always parallel to the major axis of the elliptic input beam]. The elliptic input beam [Fig. 3(d)] of $\Delta x = 32 \mu\text{m}$,

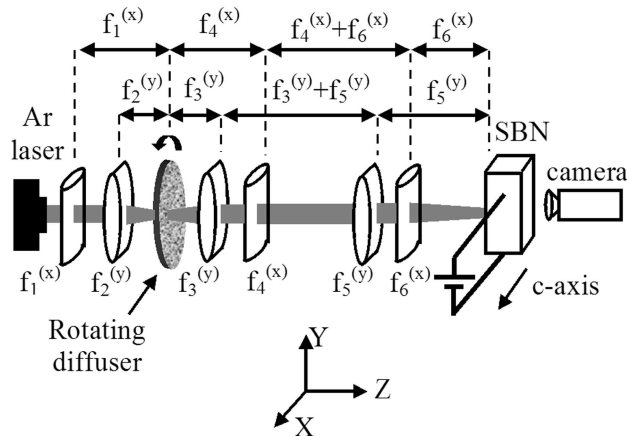


Fig. 1. Experimental setup. Note that each cylindrical lens has a superscript that signifies its focusing direction; e.g. cylindrical lens $f_1^{(x)}$ has focal length f_1 in the x direction.

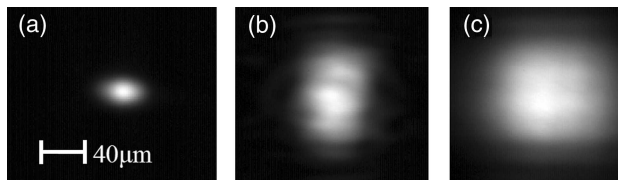


Fig. 2. Free-space diffraction of an elliptic beam. A coherent elliptic beam with input intensity structure (a) exhibits an elliptic far field rotated by 90° after 5-mm free-space diffraction (b). An elliptic incoherent beam with anisotropic correlation statistics and the input intensity structure of (a) exhibits a circular far field after propagating the same distance (c).

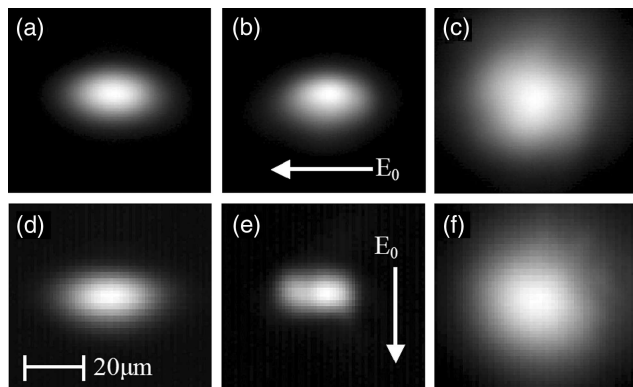


Fig. 3. Propagation of the elliptic incoherent beam with anisotropic correlation statistics in a 6-mm-long nonlinear crystal. Photographs of the input and output beams are shown. Input beam (a) forms an elliptic soliton (b) at 1.1 kV/cm. For comparison, if the nonlinearity is set to zero, the same input beam exhibits an almost ideally circular diffraction (c). In (d)–(f) the experiment of (a)–(c) is repeated but with the beam rotated by 90° with respect to the applied field, proving that the elliptic incoherent solitons do not arise from the small residual anisotropy associated with the screening nonlinearity. The directions of the applied field in (b) and (e) are indicated by arrows.

$\Delta y = 16 \mu\text{m}$ self-trapped (at 2.76 kV/cm) into an elliptic soliton $\Delta x = 28 \mu\text{m}$, $\Delta y = 14 \mu\text{m}$ [Fig. 3(e)], whereas when the nonlinearity was set to zero the beam displayed nearly circular diffraction [Fig. 3(f)], with $\Delta x = 44 \mu\text{m}$ and $\Delta y = 42 \mu\text{m}$, in spite of its elliptical (near-field) shape. The fact that we were able to generate highly eccentric elliptic solitons at both orientations, parallel to the applied field direction and perpendicular to it, proves that the main self-trapping effects that underlie the elliptic solitons do not arise from the small residual anisotropy associated with the screening nonlinearity.

In conclusion, we have demonstrated experimentally the formation of elliptic incoherent spatial solitons. We have shown that, when the correlation function of such an elliptic beam is appropriately made anisotropic, the beam has a circular far field and thus can be self-trapped in a noninstantaneous saturable nonlinearity and form an elliptic soliton.

This study is part of the Multidisciplinary University Research Initiative project on spatial solitons and was also supported by the USA–Israel Binational Science Foundation, by the German–Israeli Project Cooperation Program (DIP), and by the Israeli Science Foundation.

References

1. S. Trillo and W. Torruellas, eds., *Spatial Solitons* (Springer-Verlag, Berlin, 2001).
2. G. I. Stegeman and M. Segev, *Science* **286**, 1518 (1999).
3. J. E. Bjorkholm and A. Ashkin, *Phys. Rev. Lett.* **32**, 129 (1974).
4. G. C. Duree, J. L. Shultz, G. Salamo, M. Segev, A. Yariv, B. Crosignani, P. Di Porto, E. Sharp, and R. R. Neurgaonkar, *Phys. Rev. Lett.* **71**, 533 (1993).
5. M. Shih, M. Segev, G. C. Valley, and G. Salamo, B. Crosignani, P. Di Porto, *Electron. Lett.* **31**, 826 (1995).
6. W. E. Torruellas, Z. Wang, D. J. Hagan, E. W. Van Stryland, G. I. Stegeman, L. Torner, and C. R. Menyuk, *Phys. Rev. Lett.* **74**, 5036 (1995).
7. V. Tikhonenko, J. Christou, and B. Luther-Davies, *Phys. Rev. Lett.* **76**, 2698 (1996).
8. M. Shih, P. Leach, M. Segev, M. H. Garrett, G. Salamo, and G. C. Valley, *Opt. Lett.* **21**, 324 (1996).
9. B. Crosignani and P. Di Porto, *Opt. Lett.* **18**, 1394 (1993).
10. A. W. Snyder and J. D. Mitchell, *Opt. Lett.* **22**, 16 (1997).
11. V. Tikhonenko, *Opt. Lett.* **23**, 594 (1998).
12. M. Mitchell, Z. Chen, M. Shih, and M. Segev, *Phys. Rev. Lett.* **77**, 490 (1996).
13. M. Mitchell and M. Segev, *Nature* **387**, 880 (1997).
14. Z. Chen, M. Mitchell, M. Segev, T. Coskun, and D. N. Christodoulides, *Science* **280**, 889 (1998).
15. D. N. Christodoulides, T. H. Coskun, M. Mitchell, and M. Segev, *Phys. Rev. Lett.* **78**, 646 (1997).
16. M. Mitchell, M. Segev, T. H. Coskun, and D. N. Christodoulides, *Phys. Rev. Lett.* **79**, 4990 (1997).
17. D. N. Christodoulides, E. Eugenieva, T. Coskun, M. Segev, and M. Mitchell, *Phys. Rev. E* **63**, R35601 (2001).
18. M. Segev and D. N. Christodoulides, in *Spatial Solitons*, S. Trillo and W. Torruellas, eds. (Springer-Verlag, Berlin, 2001).
19. D. N. Christodoulides, T. H. Coskun, M. Mitchell, and M. Segev, *Phys. Rev. Lett.* **80**, 2310 (1998).
20. E. D. Eugenieva, D. N. Christodoulides, and M. Segev, *Opt. Lett.* **25**, 972 (2000).
21. W. Krolikowski, D. Edmundson, and O. Bang, *Phys. Rev. E* **61**, 3122 (2000).
22. H. Buljan, A. Siber, M. Soljacic, T. Schwartz, M. Segev, and D. N. Christodoulides, *Phys. Rev. E* **68**, 036607 (2003).
23. M. Segev, G. C. Valley, B. Crosignani, P. Di Porto, and A. Yariv, *Phys. Rev. Lett.* **73**, 3211 (1994).
24. D. N. Christodoulides and M. I. Carvalho, *J. Opt. Soc. Am. B* **12**, 1628 (1995).
25. M. Segev, M. Shih, and G. C. Valley, *J. Opt. Soc. Am. B* **13**, 706 (1996).
26. N. Korneeve, P. A. Marquez Aguilar, J. J. Sánchez Mondragón, S. Stepanov, M. Klein, and B. Wechsler, *J. Mod. Opt.* **43**, 311 (1996).
27. S. Gatz and J. Herrmann, *Opt. Lett.* **23**, 1176 (1998).